

## N-Heterocyclic Silylene

## A Stable N-Heterocyclic Silylene with a 1,1'-Ferrocenediyl Backbone

Nadine Weyer, Myron Heinz, Julia I. Schweizer, Clemens Bruhn, Max C. Holthausen,\* and Ulrich Siemeling\*

Dedicated to Professor Peter Jutzi on the occasion of his 82nd birthday

**Abstract:** The N-heterocyclic silylene  $[[\text{Fe}(\eta^5\text{-C}_5\text{H}_4\text{-NDipp})_2\text{Si}]$  (**1DippSi**, Dipp = 2,6-diisopropylphenyl) shows an excellent combination of pronounced thermal stability and high reactivity towards small molecules. It reacts readily with  $\text{CO}_2$  and  $\text{N}_2\text{O}$ , respectively affording  $(\text{1DippSiO}_2)_2\text{C}$  and  $(\text{1DippSiO})_2$  as follow-up products of the silanone **1DippSiO**. Its reactions with  $\text{H}_2\text{O}$ ,  $\text{NH}_3$ , and  $\text{FcPH}_2$  (Fc = ferrocenyl) furnish the respective oxidative addition products **1DippSi(H)X** (X = OH,  $\text{NH}_2$ , PHFc). Its reaction with  $\text{H}_3\text{BNH}_3$  unexpectedly results in B–H, instead of N–H, bond activation, affording **1DippSi(H)(BH<sub>2</sub>NH<sub>3</sub>)**. DFT results suggest that dramatically different mechanisms are operative for these H–X insertions.

The N-heterocyclic silylene (NHSi) **A**<sup>[1]</sup> (Figure 1) is a heavier NHC<sup>[2]</sup> analogue and represents the first stable compound containing divalent and dicoordinate silicon.<sup>[3]</sup> Backbone-saturated congeners are significantly more reactive. For example, whereas 1,3-bis(2,6-diisopropylphenyl)imidazolin-2-ylidene (IPr) is inert towards  $\text{PH}_3$ , the backbone-saturated congener SIPr readily inserts into a P–H bond,<sup>[4]</sup> and silylene **B** undergoes self-insertion into an Si–N bond during its tetramerisation.<sup>[5]</sup> The first isolable dialkylsilylene **C**<sup>[6]</sup> exhibits a more pronounced ambiphilicity than diaminosilylenes and rearranges to a  $\text{Si}^{\text{IV}}$  compound.<sup>[7]</sup>

The rapid development of carbene chemistry has led to acyclic diaminocarbenes (ADACs),<sup>[8]</sup> ring-expanded NHCs (reNHCs) with ring sizes  $> 5$ <sup>[9]</sup> and cyclic (alkyl)-(amino)carbenes (CAACs),<sup>[10]</sup> which are all closely related to standard NHCs, but exhibit a more pronounced ambiphilicity, and hence higher reactivity.<sup>[11]</sup> While more than a dozen

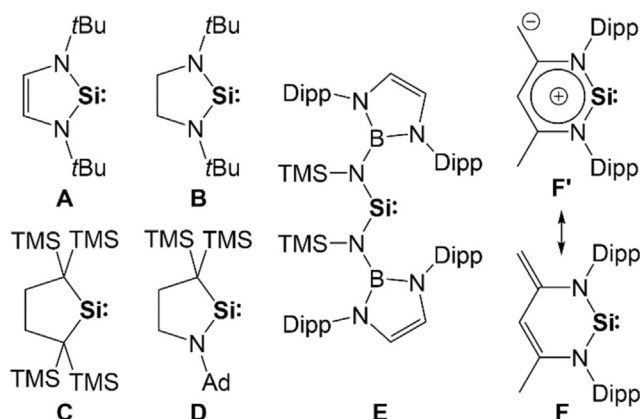


**Figure 1.** Silylenes A–F (Ad = 1-adamantyl, Dipp = 2,6-diisopropylphenyl, TMS = trimethylsilyl).

silicon analogues of standard NHCs have been isolated,<sup>[3,12]</sup> only a single example each has been reported for stable silicon analogues of CAACs,<sup>[13]</sup> ADACs<sup>[14]</sup> and reNHCs,<sup>[15]</sup> viz. silylenes **D–F** (Figure 1). The ambivalent reactivity of reNHSi **F** was rationalised by a significant contribution of N-ylidic canonical structures summarised as **F'**. We here report on the reNHSi  $[[\text{Fe}(\eta^5\text{-C}_5\text{H}_4\text{-NDipp})_2\text{Si}]$  (**1DippSi**), which contains a six-membered  $\text{FeC}_2\text{N}_2\text{Si}$  ring. **1DippSi** is an analogue of our stable ferrocene-based NHCs, whose ambiphilicity allowed for small-molecule activation reactions unprecedented for diaminocarbenes.<sup>[16,17]</sup>

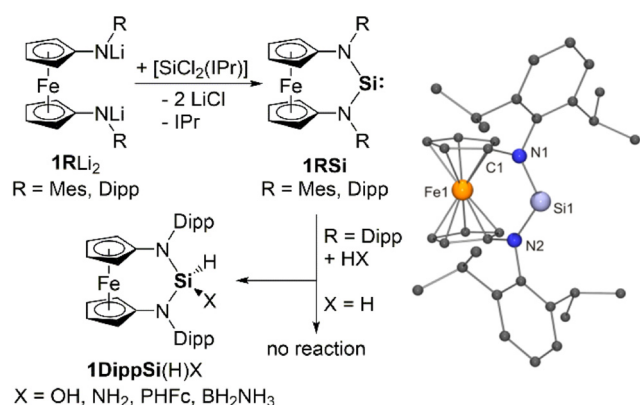
Our attempts to obtain reNHSis of the type **1RSi** by reduction of corresponding  $\text{Si}^{\text{IV}}$  dihalides **1RSiX<sub>2</sub>** (X = Cl, Br) or by  $\alpha$ -elimination of HCl from **1RSi(H)Cl** were unsuccessful.<sup>[18]</sup> An alternative approach, which was introduced for the acyclic diaminosilylene (ADASI) **E**, is the reaction of  $[\text{SiCl}_2\text{-IPr}]$ <sup>[19]</sup> with the corresponding lithium amide.<sup>[14]</sup> This  $\text{Si}^{\text{II}}$  precursor turned out to be the key to success. Its reaction with **1MesLi<sub>2</sub>** in  $\text{C}_6\text{D}_6$  afforded the silylene **1MesSi** together with IPr (Scheme 1). Although too unstable for isolation, **1MesSi** was sufficiently persistent at room temperature for detecting its <sup>29</sup>Si NMR signal ( $\delta = 121.5$  ppm), which is significantly downfield-shifted with respect to reNHSi **F** ( $\delta = 88.4$  ppm)<sup>[15]</sup> and NHSi **A** (78.3 ppm).<sup>[1]</sup> The signal of the  $\text{Si}^{\text{II}}$  atom in ADASI **E** was observed at even lower field ( $\delta = 204.6$  ppm).<sup>[14]</sup> Trapping of **1MesSi** with  $(\text{PhSe})_2$  at room temperature in benzene solution afforded **1MesSi(SePh)<sub>2</sub>**; details are provided in the Supporting Information (SI). The bulkier homologue **1DippSi**, obtained from  $[\text{SiCl}_2(\text{IPr})]$  and **1DippLi<sub>2</sub>** in toluene at room temperature, is sufficiently stable

[\*] N. Weyer, Dr. C. Bruhn, Prof. Dr. U. Siemeling  
Institut für Chemie, Universität Kassel  
Heinrich-Plett-Straße 40, 34132 Kassel (Germany)  
E-mail: siemeling@uni-kassel.de

M. Heinz, Dr. J. I. Schweizer, Prof. Dr. M. C. Holthausen  
Institut für Anorganische und Analytische Chemie, Goethe-Universität  
Max-von-Laue-Straße 7, 60438 Frankfurt am Main (Germany)  
E-mail: max.holthausen@chemie.uni-frankfurt.de

Supporting information and the ORCID identification number(s) for the author(s) of this article can be found under:  
<https://doi.org/10.1002/anie.202011691>.

© 2020 The Authors. Angewandte Chemie International Edition published by Wiley-VCH GmbH. This is an open access article under the terms of the Creative Commons Attribution License, which permits use, distribution and reproduction in any medium, provided the original work is properly cited.



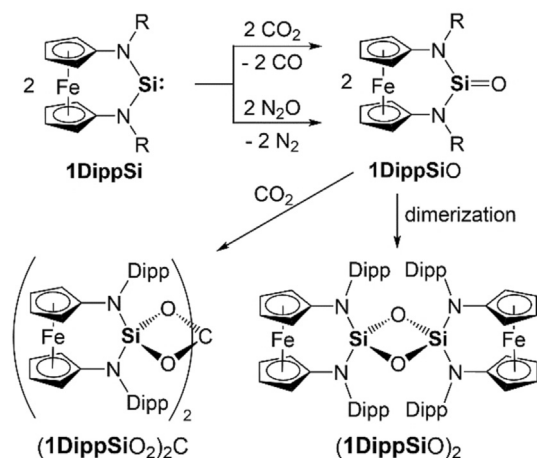
**Scheme 1.** Synthesis of **1MesSi** (persistent, Mes = mesityl) and **1DippSi** (stable) and reactions of the latter with H<sub>2</sub>O, NH<sub>3</sub>, FcPH<sub>2</sub> (Fc = ferrocenyl), and H<sub>3</sub>BNH<sub>3</sub> under ambient conditions in benzene or toluene. Selected bond lengths [Å] and angles [°] for **1DippSi**: Si1-N1 1.7327(12), Si1-N2 1.7344(12), N1-Si1-N2 106.58(6); sum of angles ( $\Sigma\angle$ ) at N1 359.9, at N2 360.0.

for isolation (Scheme 1). IPr and **1DippSi** could not be separated by crystallisation or sublimation. It was possible to remove IPr from ADASi **E** by stirring a hexane solution of the mixture at room temperature under an atmosphere of CO<sub>2</sub>, which led to the precipitation of IPr(CO<sub>2</sub>).<sup>[14]</sup> This method was not successful in our case, because, in contrast to **E**, **1DippSi** reacts swiftly with CO<sub>2</sub> under the same mild conditions, affording the orthocarbonate (**1DippSiO<sub>2</sub>**)<sub>2</sub>C (Scheme 2; see the SI). The primary products are most likely CO and the silanone **1DippSiO**,<sup>[20]</sup> which subsequently undergoes a cycloaddition with CO<sub>2</sub> in a 2:1 ratio. When generated by reaction of **1DippSi** with N<sub>2</sub>O in benzene at room temperature, this silanone forms the expected dimer (**1DippSiO**)<sub>2</sub> (Scheme 2; see the SI).<sup>[21]</sup> An analogous stepwise reaction with CO<sub>2</sub> was first reported for decamethylsilicocene (Cp\*<sub>2</sub>Si).<sup>[22]</sup> Dialkylsilylene **C**<sup>[23]</sup> as well as IPr = N-Si-OSi<sup>t</sup>Bu<sub>3</sub> and IPr = N-Si-Si(SiMe<sub>3</sub>)<sub>3</sub>, an acyclic (imino)(siloxy)- and (imino)(silyl)silylene,<sup>[24]</sup> are the only examples containing dicoordi-

nate Si<sup>II</sup> in this context to date.<sup>[25]</sup> We found that IPr is easily removed by complexation with ZnCl<sub>2</sub>, which is inert towards **1DippSi**. In contrast to **1DippSi**, [ZnCl<sub>2</sub>(IPr)]<sup>[26]</sup> is insoluble in hexane.

The <sup>29</sup>Si NMR signal of **1DippSi** is located at  $\delta = 115.7$  ppm, upfield-shifted by 6 ppm with respect to **1MesSi**. **1DippSi** was structurally characterised by X-ray diffraction (Scheme 1). The Si bond angle (106.6°) lies in between the values determined for reNHSi **F** (99.3°)<sup>[15]</sup> and ADASi **E** (110.9°)<sup>[14]</sup> and is close to that reported for a heterocyclic silylene with a six-membered ring containing an NSi<sup>II</sup>BP unit.<sup>[27]</sup> Silylenes whose dicoordinate Si<sup>II</sup> atom is part of a five-membered ring exhibit more acute Si bond angles close to 90°.<sup>[3,6,12,13,28]</sup>

Similar to **1MesSi**, **1DippSi** undergoes an oxidative addition with (PhSe)<sub>2</sub> in benzene solution at room temperature to afford **1DippSi(SePh)<sub>2</sub>** (see the SI). We next addressed the oxidative addition of strong H-X bonds of different polarities, which is of fundamental importance for chemical synthesis and catalysis.<sup>[29]</sup> While **1DippSi** is inert towards H<sub>2</sub> under ambient conditions, it reacted readily with H<sub>2</sub>O, NH<sub>3</sub>, and FcPH<sub>2</sub>, affording the corresponding derivatives of the type **1DippSi(H)X** (Scheme 1, Figure 2; X = OH, NH<sub>2</sub>, PHFc; see the SI). The reaction of H<sub>2</sub>O with stable dicoordinate Si<sup>II</sup> compounds to the corresponding hydroxysilane has been reported only for the metallasilylene [Cp\*-(CO)<sub>3</sub>Cr-Si-SiPr]<sup>+</sup><sup>[30]</sup> as well as for **A**<sup>[31]</sup> and **F**.<sup>[32]</sup> The hydroxysilanes **A(H)OH** and **F(H)OH** were not observed, but their intermediacy was merely inferred from the products isolated. In contrast, the analogous NH<sub>3</sub> addition product **F(H)NH<sub>2</sub>** was obtained in high yield from the reaction of **F** with NH<sub>3</sub>.<sup>[33]</sup> **F** is the exception to the rule that five- and six-membered NHSis cannot be employed for NH<sub>3</sub> activation, although they are more Lewis acidic and have a smaller singlet-triplet gap compared to the corresponding NHCs.<sup>[34]</sup> Apart from [Cp\*-(CO)<sub>3</sub>Cr-Si-SiPr]<sup>+</sup>,<sup>[30]</sup> Dipp(Me<sub>3</sub>Si)N-Si-Si(SiMe<sub>3</sub>)<sub>3</sub><sup>[35]</sup> and IPr = N-Si-OSi<sup>t</sup>Bu<sub>3</sub><sup>[24a]</sup> we are not aware of any other stable silylene to undergo an oxidative addition of NH<sub>3</sub>. The reaction of NH<sub>3</sub> with **1DippSi** is remarkable



**Scheme 2.** Reactions of **1DippSi** with CO<sub>2</sub> and N<sub>2</sub>O under ambient conditions in benzene, respectively affording (**1DippSiO<sub>2</sub>**)<sub>2</sub>C and (**1DippSiO**)<sub>2</sub> via the silanone **1DippSiO** as assumed intermediate.

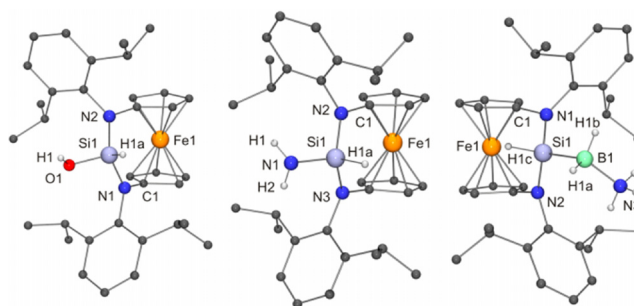


**Figure 2.** Molecular structures of **1DippSi(H)OH** (left; selected bond lengths [Å] and angles [°]: Si1-N1 1.7197(16), Si1-N2 1.7199(16), Si1-O1 1.6071(16), N1-Si1-N2 111.49(8);  $\Sigma\angle$  at N1 359.9, at N2 359.4), **1DippSi(H)NH<sub>2</sub>** (middle; selected bond lengths [Å] and angles [°]: Si1-N1 1.691(4), Si1-N2 1.721(3), Si1-N3 1.730(3), N2-Si1-N3 111.72(14);  $\Sigma\angle$  at N2 358.5, at N3 358.0) and **1DippSi(H)(BH<sub>2</sub>NH<sub>3</sub>)** (right; selected bond lengths [Å] and angles [°]: Si1-N1 1.7571(14), Si1-N2 1.7694(14), Si1-B1 2.008(2), N3-B1 1.600(3), N1-Si1-N2 107.84(7), Si1-B1-N1 116.41(13);  $\Sigma\angle$  at N1 358.3, at N2 356.6).

because  $\text{NH}_3$  activation is a challenging target even for transition metal complexes<sup>[36]</sup>—the potential of low-valent main-group element compounds in this context was uncovered only recently.<sup>[25,37]</sup> The reaction of **1DippSi** with  $\text{FcPH}_2$  afforded the oxidative addition product **1DippSi(H)(PHFc)**. In view of the ability of **1DippSi** for N–H activation, the activation of a P–H bond, which is weaker than an N–H bond by ca.  $100 \text{ kJ mol}^{-1}$ , is not unexpected;<sup>[38]</sup>  $\text{reNHSi F}$  is also capable of P–H activation.<sup>[39]</sup> We next addressed the reaction of **1DippSi** with  $\text{H}_3\text{BNH}_3$  (Scheme 1),<sup>[40]</sup> expecting the formation of **1DippSiH<sub>2</sub>**, most likely by transfer of a protic and a hydridic H atom<sup>[41]</sup> to the divalent atom, as was observed for 1,3-di-*tert*-butylimidazolin-2-ylidene<sup>[33]</sup> and  $\text{reNHSi F}$ .<sup>[42]</sup> Instead, the reaction furnished **1DippSi(H)-(BH<sub>2</sub>NH<sub>3</sub>)** (Figure 2), although the B–H bond is stronger than the N–H bond of  $\text{H}_3\text{BNH}_3$ .<sup>[43]</sup> First B–H bond activation reactions with  $\text{Si}^{\text{II}}$  compounds were reported only recently,<sup>[44]</sup> and the reaction of the (silyl)-(vinyl)silylene  $\text{Me}^e\text{IPr} = \text{CH-Si-Si}(\text{SiMe}_3)_3$  ( $\text{Me}^e\text{IPr} = 1,3\text{-bis}(2,6\text{-diisopropylphenyl})\text{-4,5-dimethylimidazolin-2-ylidene}$ ) with pinacolborane (HBPIn), which affords  $\text{Me}^e\text{IPr} = \text{CH-Si(H)-(Bpin)-Si}(\text{SiMe}_3)_3$ , is the only example involving dicoordinate  $\text{Si}^{\text{II}}$ .<sup>[45]</sup>

We performed a DFT study on the electronic characteristics and the reactivity of **1**, the full molecular model of **1DippSi**.<sup>[46]</sup> At the PBEh-3c level of DFT employed, the HOMO comprises the expected silylene lone pair together with significant contributions of the ferrocene moiety and the LUMO is dominated by the silylene p-orbital, with a substantial HOMO–LUMO energy separation of  $\Delta E_{\text{H/L}} = 6.4 \text{ eV}$ . The unexpectedly low computed singlet–triplet energy difference of  $\Delta E_{\text{S/T}} = 0.4 \text{ eV}$  does not correlate with this value because the lowest triplet state arises from a local excitation within the ferrocene moiety and does not involve the silylene p-orbital (Figure 3).<sup>[47]</sup>

Surprisingly, direct oxidative addition of  $\text{H}_2\text{O}$  and  $\text{NH}_3$  to **1** is precluded by high kinetic barriers for both substrates ( $35$  and  $42 \text{ kcal mol}^{-1}$ , respectively), and two distinct alternative pathways were identified instead. The lowest-energy pathway for  $\text{NH}_3$  activation commences with the formation of adduct **2** (Scheme 3, top). Proton transfer is facilitated by a second  $\text{NH}_3$  molecule acting as a proton shuttle and the experimentally observed product **3** is formed in a strongly exergonic step with a moderate overall barrier of  $20 \text{ kcal mol}^{-1}$ .  $\text{H}_2\text{O}$ , in turn, does not form a datively bonded adduct with **1**, but directly adds across an Si–N bond via **TS2** to form hydroxysilylene **4** in an exergonic step (Scheme 3, bottom). From there on out,

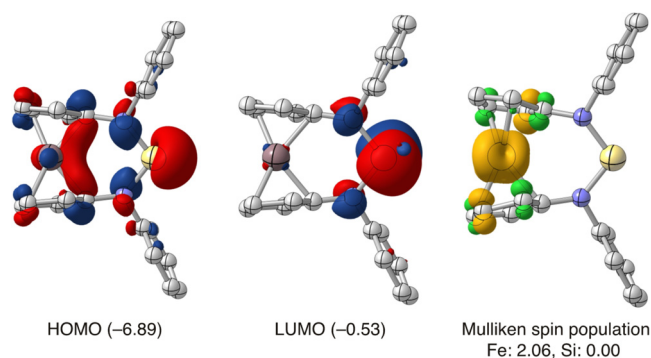
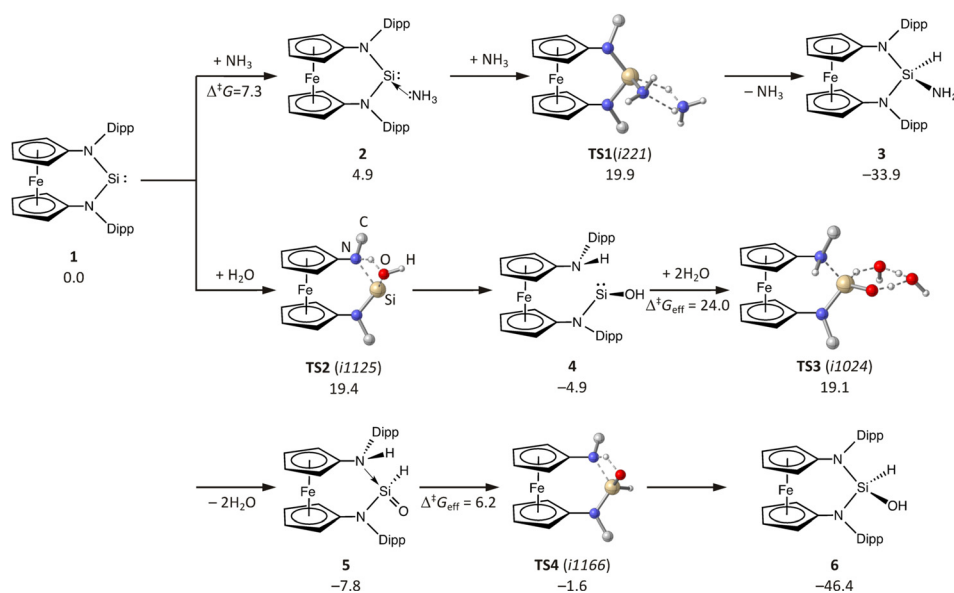


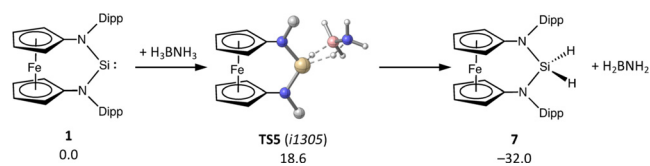
**Figure 3.** Frontier molecular orbitals and triplet spin-density distribution computed for **1** (i. e. the full molecular model of **1DippSi**; orbital energies in eV, isocontour surfaces at  $\pm 0.05 \text{ a}_0^{-3/2}$  for orbitals and  $\pm 0.005 \text{ a}_0^{-3}$  for the spin density,  $\alpha$  spin: yellow,  $\beta$  spin: green; *iPr* groups and H atoms not shown).



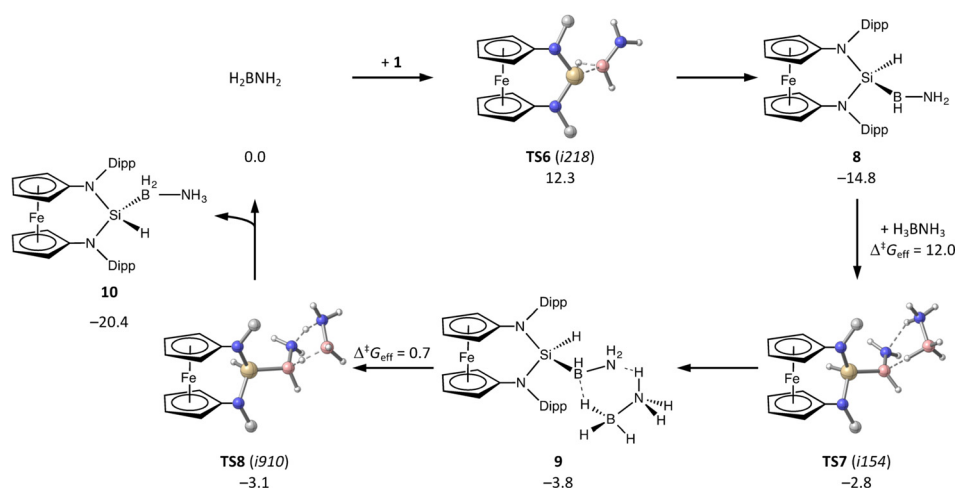
**Scheme 3.** Computed lowest-energy reaction pathway for the formal H–X oxidative addition to **1** with  $\text{NH}_3$  (top) and  $\text{H}_2\text{O}$  (bottom,  $\Delta G^{298}$  in  $\text{kcal mol}^{-1}$ ). Bonds formed or broken in transition states are dashed, unreactive H atoms are omitted and the orientation of the Dipp substituents in the transition state is indicated by showing the respective  $\text{C}_{\text{ipso}}$  atom only.

silanone **5** is formed through a water-assisted proton transfer;<sup>[48]</sup> the experimentally observed product **6** results in a strongly exergonic step after passage of a minute barrier in **TS4**.

The quantum-chemical evaluation discloses a concerted dehydrogenation of  $\text{H}_3\text{BNH}_3$  by **1** as initial step along the lowest-energy pathway for ammonia-borane activation (Scheme 4). Alternative direct insertion of **1** into an N–H



**Scheme 4.** Computed reaction path for the formation of **7** from **1** and  $\text{H}_3\text{BNH}_3$ ;  $\Delta G^{298}$  in  $\text{kcal mol}^{-1}$ .



**Scheme 5.** Computed reaction path for the formation of **10** from **1**,  $\text{H}_2\text{BNH}_2$  and  $\text{H}_3\text{BNH}_3$  ( $\Delta G^{298}$  in  $\text{kcal mol}^{-1}$  relative to the separated reactants, activation barriers relative to the preceding minimum).

or B–H bond is precluded by high kinetic barriers (53 and 35  $\text{kcal mol}^{-1}$ , respectively; see the SI). Whereas the resulting silane **7** forms as an unreactive side product,<sup>[49]</sup>  $\text{H}_2\text{BNH}_2$  is a highly reactive species that has been thoroughly studied in the thermal and catalytic dehydrogenation of  $\text{H}_3\text{BNH}_3$  and is known to polymerize below  $-150^\circ\text{C}$ .<sup>[50]</sup>

Obviously, B–H insertion of **1** in  $\text{H}_2\text{BNH}_2$  competes efficiently with the polymerization of the latter, leading to the formation of **8** (Scheme 5). With a low barrier of 12  $\text{kcal mol}^{-1}$  **8** can dehydrogenate a second equivalent of  $\text{H}_3\text{BNH}_3$  through intermediate **9** yielding the experimentally observed product **10** while regenerating  $\text{H}_2\text{BNH}_2$ . After initial formation of  $\text{H}_2\text{BNH}_2$  from **1** and  $\text{H}_3\text{BNH}_3$  the follow-up reaction cascade involving B–H insertion by **1** and subsequent dehydrogenation of  $\text{H}_3\text{BNH}_3$  is kinetically favoured over the formation of **7**.

In conclusion, we have described the synthesis and reactivity of the new stable reNHSi **1DippSi**. **1DippSi** reacts readily with  $\text{N}_2\text{O}$  and  $\text{CO}_2$ , which is in contrast to the inertness of **F**, the only other stable cyclic diaminosilylene featuring a ring-expanded structure known to date.<sup>[25a]</sup> Studies on the reactivity of **1DippSi** towards H–X bonds of different strengths and polarities show parallels to previous reactivity studies on other silylenes. The reactions with  $\text{NH}_3$  and  $\text{H}_2\text{O}$  both give the H–X insertion products. Mechanistically, however, they differ significantly. More particularly, the lowest-energy path of the reaction with  $\text{H}_2\text{O}$  involves the N–Si cooperative activation of an O–H bond. For  $\text{H}_3\text{BNH}_3$  the reaction mechanism consists of two key elementary steps, the first one being the dehydrogenation of  $\text{H}_3\text{BNH}_3$  to  $\text{H}_2\text{BNH}_2$ , which subsequently catalyses the conversion of **1DippSi** to **1DippSi(H)(BH<sub>2</sub>NH<sub>3</sub>)** with  $\text{H}_3\text{BNH}_3$ . In contrast to  $\text{H}_3\text{BNH}_3$ ,  $\text{H}_2\text{BNH}_2$  has a vacant p-orbital, which enables insertion of the silylene in a B–H bond in the second step. This silylborane can in turn dehydrogenate a second equivalent of  $\text{H}_3\text{BNH}_3$  to give the final product **1DippSi(H)(BH<sub>2</sub>NH<sub>3</sub>)**.

## Acknowledgements

Quantum-chemical were performed at the Center for Scientific Computing (CSC) Frankfurt on the Goethe and Fuchs high-performance compute clusters. Open access funding enabled and organized by Projekt DEAL.

## Conflict of interest

The authors declare no conflict of interest.

**Keywords:** carbenehomologues · insertion · metallocenes · silicon · subvalent compounds

- [1] M. Denk, R. Lennon, R. Hayashi, R. West, A. V. Belyakov, H. P. Verne, A. Haaland, M. Wagner, N. Metzler, *J. Am. Chem. Soc.* **1994**, *116*, 2691–2692.
- [2] M. N. Hopkinson, C. Richter, M. Schedler, F. Glorius, *Nature* **2014**, *510*, 485–496.
- [3] M. Asay, C. Jones, M. Driess, *Chem. Rev.* **2011**, *111*, 354–396.
- [4] M. Bispinghoff, A. M. Tondreau, H. Grützmacher, C. A. Faradji, P. G. Pringle, *Dalton Trans.* **2016**, *45*, 5999–6003.
- [5] T. A. Schmedake, M. Haaf, Y. Apeloig, T. Müller, S. Bukalov, R. West, *J. Am. Chem. Soc.* **1999**, *121*, 9479–9480.
- [6] M. Kira, S. Ishida, T. Iwamoto, C. Kabuto, *J. Am. Chem. Soc.* **1999**, *121*, 9722–9723.
- [7] M. Kira, *Chem. Commun.* **2010**, *46*, 2893–2903.
- [8] a) V. P. Boyarskiy, K. V. Luzyanin, V. Y. Kukushkin, *Coord. Chem. Rev.* **2012**, *256*, 2029–2056; b) L. M. Slaughter, *ACS Catal.* **2012**, *2*, 1802–1816; c) J. Vignolle, X. Cattoën, D. Bourissou, *Chem. Rev.* **2009**, *109*, 3333–3384.
- [9] a) X. Yong, R. Thurston, C.-Y. Ho, *Synthesis* **2019**, *51*, 2058–2080; b) J. Li, W.-x. Shen, X.-r. Li, *Curr. Org. Chem.* **2013**, *16*, 2879–2891.
- [10] a) M. Melaimi, R. Jazzar, M. Soleilhavoup, G. Bertrand, *Angew. Chem. Int. Ed.* **2017**, *56*, 10046–10068; *Angew. Chem.* **2017**, *129*, 10180–10203; b) M. Soleilhavoup, G. Bertrand, *Acc. Chem. Res.* **2015**, *48*, 256–266.
- [11] a) D. Munz, *Organometallics* **2018**, *37*, 275–289; b) D. Martin, Y. Canac, V. Lavallo, G. Bertrand, *J. Am. Chem. Soc.* **2014**, *136*, 5023–5030.
- [12] a) L. Zhu, J. Zhang, C. Cui, *Inorg. Chem.* **2019**, *58*, 12007–12010; b) I. L. Fedushkin, A. N. Lukoyanov, N. M. Khvoynova, A. V. Cherkasov, *Russ. Chem. Bull.* **2013**, *62*, 2454–2461; c) P. Zark, A. Schäfer, A. Mitra, D. Haase, W. Saak, R. West, T. Müller, *J. Organomet. Chem.* **2010**, *695*, 398–408.
- [13] T. Kosai, S. Ishida, T. Iwamoto, *Angew. Chem. Int. Ed.* **2016**, *55*, 15554–15558; *Angew. Chem.* **2016**, *128*, 15783–15787.
- [14] T. J. Hadlington, J. A. B. Abdalla, R. Tirfoin, S. Aldridge, C. Jones, *Chem. Commun.* **2016**, *52*, 1717–1720.
- [15] M. Driess, S. Yao, M. Brym, C. van Wüllen, D. Lentz, *J. Am. Chem. Soc.* **2006**, *128*, 9628–9629.
- [16] a) A. R. Petrov, A. Derheim, J. Oetzel, M. Leibold, C. Bruhn, S. Scheerer, S. Obwald, R. F. Winter, U. Siemeling, *Inorg. Chem.* **2015**, *54*, 6657–6670; b) U. Siemeling, C. Färber, C. Bruhn, M.

- Leibold, D. Selent, W. Baumann, M. von Hopffgarten, C. Goedecke, G. Frenking, *Chem. Sci.* **2010**, *1*, 697–704.
- [17] a) R. Guthardt, J. Oetzel, J. I. Schweizer, C. Bruhn, R. Langer, M. Maurer, J. Vícha, P. Shestakova, M. C. Holthausen, U. Siemeling, *Angew. Chem. Int. Ed.* **2019**, *58*, 1387–1391; *Angew. Chem.* **2019**, *131*, 1401–1405; b) J. Oetzel, N. Weyer, C. Bruhn, M. Leibold, B. Gerke, R. Pöttgen, M. Maier, R. F. Winter, M. C. Holthausen, U. Siemeling, *Chem. Eur. J.* **2017**, *23*, 1187–1199.
- [18] J. Oetzel, C. Bruhn, U. Siemeling, *Z. Anorg. Allg. Chem.* **2018**, *644*, 935–944.
- [19] R. S. Ghadwal, H. W. Roesky, S. Merkel, J. Henn, D. Stalke, *Angew. Chem. Int. Ed.* **2009**, *48*, 5683–5686; *Angew. Chem.* **2009**, *121*, 5793–5796.
- [20] Recent examples for oxygenations of stable low-valent Si compounds with CO<sub>2</sub>: a) A. V. Protchenko, P. Vasko, D. Cao Huan Do, J. Hicks, M. Á. Fuentes, C. Jones, S. Aldridge, *Angew. Chem. Int. Ed.* **2019**, *58*, 1808–1812; *Angew. Chem.* **2019**, *131*, 1822–1826; b) A. Burchert, S. Yao, R. Müller, C. Schattner, Y. Xiong, M. Kaupp, M. Driess, *Angew. Chem. Int. Ed.* **2017**, *56*, 1894–1897; *Angew. Chem.* **2017**, *129*, 1920–1923; c) Y. Wang, M. Chen, Y. Xie, P. Wei, H. F. Schaefer III, G. H. Robinson, *J. Am. Chem. Soc.* **2015**, *137*, 8396–8399; d) F. M. Mück, J. A. Baus, M. Nutz, C. Burschka, J. Poater, F. M. Bickelhaupt, R. Tacke, *Chem. Eur. J.* **2015**, *21*, 16665–16672.
- [21] W. Li, N. J. Hill, A. C. Tomasik, G. Bikzhanova, R. West, *Organometallics* **2006**, *25*, 3802–3805.
- [22] P. Jutzi, D. Eikenberg, A. Möhrke, B. Neumann, H.-G. Stammler, *Organometallics* **1996**, *15*, 753–759.
- [23] X. Liu, X.-Q. Xiao, Z. Xu, X. Yang, Z. Li, Z. Dong, C. Yan, G. Lai, M. Kira, *Organometallics* **2014**, *33*, 5434–5439.
- [24] a) D. Reiter, P. Frisch, D. Wendel, F. Hörmann, S. Inoue, *Dalton Trans.* **2020**, *49*, 7060–7068; b) D. Wendel, A. Porzelt, F. A. D. Herz, D. Sarkar, C. Jandl, S. Inoue, B. Rieger, *J. Am. Chem. Soc.* **2017**, *139*, 8134–8137.
- [25] a) C. Shan, S. Yao, M. Driess, *Chem. Soc. Rev.* **2020**, *49*, 6733–6754; b) S. Fujimori, S. Inoue, *Eur. J. Inorg. Chem.* **2020**, 3131–3142.
- [26] O. Jacquet, X. Frogneux, C. Das Neves Gomes, T. Cantat, *Chem. Sci.* **2013**, *4*, 2127–2131.
- [27] A. Rosas-Sánchez, I. Alvarado-Beltran, A. Baceiredo, N. Saffon-Merceron, S. Massou, V. Branchadell, T. Kato, *Angew. Chem. Int. Ed.* **2017**, *56*, 10549–10554; *Angew. Chem.* **2017**, *129*, 10685–10690.
- [28] a) R. Kobayashi, S. Ishida, T. Iwamoto, *Angew. Chem. Int. Ed.* **2019**, *58*, 9425–9428; *Angew. Chem.* **2019**, *131*, 9525–9528; b) T. Abe, R. Tanaka, S. Ishida, M. Kira, T. Iwamoto, *J. Am. Chem. Soc.* **2012**, *134*, 20029–20032.
- [29] T. Chu, G. I. Nikonov, *Chem. Rev.* **2018**, *118*, 3608–3680.
- [30] A. C. Filippou, B. Baars, O. Chernov, Yu. N. Lebedev, G. Schnakenburg, *Angew. Chem. Int. Ed.* **2014**, *53*, 565–570; *Angew. Chem.* **2014**, *126*, 576–581.
- [31] M. Haaf, A. Schmiedel, T. A. Schmedake, D. R. Powell, A. J. Millevolte, M. Denk, R. West, *J. Am. Chem. Soc.* **1998**, *120*, 12714–12719.
- [32] S. Yao, M. Brym, C. van Wüllen, M. Driess, *Angew. Chem. Int. Ed.* **2007**, *46*, 4159–4162; *Angew. Chem.* **2007**, *119*, 4237–4240.
- [33] A. Jana, C. Schulzke, H. W. Roesky, *J. Am. Chem. Soc.* **2009**, *131*, 4600–4601.
- [34] A. Metzler, S. Inoue, C. Präsang, M. Driess, *J. Am. Chem. Soc.* **2010**, *132*, 3038–3046.
- [35] A. V. Protchenko, J. I. Bates, L. M. A. Saleh, M. P. Blake, A. D. Schwarz, E. L. Kolychev, A. L. Thompson, C. Jones, P. Mountford, S. Aldridge, *J. Am. Chem. Soc.* **2016**, *138*, 4555–4564.
- [36] J. Hoover, *Science* **2016**, *354*, 707–708.
- [37] a) C. Weetman, S. Inoue, *ChemCatChem* **2018**, *10*, 4213–4228; b) S. Yadav, S. Saha, S. S. Sen, *ChemCatChem* **2016**, *8*, 486–501; c) P. P. Power, *Nature* **2010**, *463*, 171–177.
- [38] E–H bond dissociation energies for EH<sub>3</sub> and MeEH<sub>2</sub> are 450 and 425 kJ mol<sup>-1</sup>, respectively, for E = N, but 351 and 322 kJ mol<sup>-1</sup>, respectively, for E = P; see: Y. R. Luo, *Comprehensive Handbook of Chemical Bond Energies*, CRC Press, Boca Raton, FL, **2007**.
- [39] C. Präsang, M. Stoelzel, S. Inoue, A. Meltzer, M. Driess, *Angew. Chem. Int. Ed.* **2010**, *49*, 10002–10005; *Angew. Chem.* **2010**, *122*, 10199–10202.
- [40] a) U. B. Demirci, *Int. J. Hydrogen Energy* **2017**, *42*, 9978–10013; b) A. Staubitz, A. P. M. Robertson, I. Manners, *Chem. Rev.* **2010**, *110*, 4079–4124.
- [41] D. H. A. Boom, A. R. Jupp, J. C. Slootweg, *Chem. Eur. J.* **2019**, *25*, 9133–9152.
- [42] M. Stoelzel, C. Präsang, S. Inoue, S. Enthaler, M. Driess, *Angew. Chem. Int. Ed.* **2012**, *51*, 399–403; *Angew. Chem.* **2012**, *124*, 411–415.
- [43] a) M. H. Matus, D. J. Grant, M. Tho Nguyen, D. A. Dixon, *J. Chem. Phys. C* **2009**, *113*, 16553–16560; b) P. R. Rablen, J. F. Hartwig, *J. Am. Chem. Soc.* **1996**, *118*, 4648–4653.
- [44] a) V. S. V. S. N. Swamy, K. V. Raj, K. Vanka, S. S. Sen, H. W. Roesky, *Chem. Commun.* **2019**, 55, 3536–3539; b) S. Khoo, Y.-L. Shan, M.-C. Yang, Y. Li, M.-D. Su, C.-W. So, *Inorg. Chem.* **2018**, *57*, 5879–5887.
- [45] M. M. D. Roy, M. J. Ferguson, R. McDonald, Y. Zhou, E. Rivard, *Chem. Sci.* **2019**, *10*, 6476–6481.
- [46] All calculations were performed with the PBEh-3c method implemented in ORCA 4.1.2. For a benchmark against F12 coupled cluster theory and further technical details see the SI.
- [47] As it is becoming commonplace to tentatively correlate  $\Delta E_{\text{H/L}}$  and/or  $\Delta E_{\text{ST}}$  of a silylene with its reactivity (see, for example, Ref. [25]), it is important to realize that both parameters exhibit a substantial method dependence (see Figure S46 in the SI), which is not commonly acknowledged in the literature. For comparison, we thus provide as SI (Figure S45) electronic characteristics evaluated at the PBEh-3c level for several silylenes published by others.
- [48] In view of Singleton's criticism, the corresponding alternative reaction paths identified are provided as SI. See: R. E. Plata, D. A. Singleton, *J. Am. Chem. Soc.* **2015**, *137*, 3811–3826.
- [49] The presence of traces of this silane in the crude product is indicated by a low-intensity <sup>29</sup>Si NMR signal at  $\delta = -34.1$  ppm (see Figure S44 in the SI), which was absent after recrystallization.
- [50] C. T. Kwon, H. A. McGee, Jr., *Inorg. Chem.* **1970**, *9*, 2458–2461.

Manuscript received: August 26, 2020

Revised manuscript received: October 1, 2020

Accepted manuscript online: October 15, 2020

Version of record online: December 1, 2020